

## Characteristics of the flight model optics for the JET-X telescope onboard the SPECTRUM X- $\gamma$ satellite

O. Citterio, S. Campana, P. Conconi, M. Ghigo, F. Mazzoleni, E. Poretti  
Osservatorio Astronomico di Brera-Milano  
Via E. Bianchi, 46 - 22055 Merate, Italy  
Tel. +39-39-9906412, Fax +39-39-9908492

G. Conti  
CNR, Istituto di Fisica Cosmica  
Via E. Bassini, 15 - 20133 Milano, Italy  
Tel. +39-2-2665237, Fax +39-2-2362946

G. Cusumano, B. Sacco  
CNR, Istituto di Fisica Cosmica  
Via M. Stabile, 172 - 90139 Palermo, Italy  
Tel. +39-91-6055364, Fax +39-91-6055355

H. Bräuninger, W. Burkert, R. Egger  
Max Planck Institut für Extraterrestrische Physik  
Giessenbachstrasse - 85748 Garching, Germany  
Tel. +49-89-7455770, Fax +49-89-74557718

C.M. Castelli, R. Willingale  
X-ray Astronomy Group, Department of Physics and Astronomy, University of Leicester  
University Road - LE1 7RH Leicester, United Kingdom  
Tel. +44-116-2523522, Fax +44-116-2523311

### ABSTRACT

The Joint European X-Ray Telescope (JET-X) is one of the core scientific instruments of the Russian SPECTRUM X- $\gamma$  astrophysics mission. JET-X is designed to study the emission from X-ray sources in the band of 0.3–10 keV; in particular to meet primary scientific goals in cosmology and extragalactic astronomy. JET-X consists of two identical, coaligned X-ray telescopes, each with a spatial resolution of better than 30 arcsec Half Energy Width. Focal plane imaging is provided by cooled X-ray sensitive CCD detectors which combine high spatial resolution with good spectral resolution, including coverage of the iron line complex around 7 keV at a resolution of  $\Delta E/E \sim 1.5\%$ . Each telescope is composed of a nested array of 12 mirror shells with an aperture of 300 mm and focal length of 3500 mm; the total effective area is 330 cm<sup>2</sup> at 1.5 keV and 145 cm<sup>2</sup> at 8.1 keV. The mirror shells have a Wolter I geometry and are manufactured by an electroforming replica process. The paper presents the characteristic of the flight model X-Ray optics.

**KEYWORDS:** X-ray optics, grazing incidence optics, X-ray telescope, JET-X

## 1 INTRODUCTION

The Joint European Telescope for X-rays (JET-X) is a collaborative project developed by a consortium of scientific institutes in the United Kingdom (Universities of Leicester and Birmingham, the Rutherford Appleton and the Mullard Space Science Laboratories), in Italy (Brera Astronomical Observatory, Palermo and Milano CNR institutes and University groups in Milano and Roma), in Germany (Max Planck Institute, Garching) and in Russia (IKI, Moscow). The JET-X telescope is one of the key instruments onboard the SPECTRUM X- $\gamma$  satellite, a scientific multi-mission satellite aimed to study astrophysical high energy sources in the X and  $\gamma$ -ray energy bands.

The JET-X telescope<sup>1</sup> has been developed to study X-ray sources in the energy range 0.3–10 keV to provide major advances in X-ray cosmology and extragalactic astronomy. The scientific requirements of JET-X were a spatial resolution better than 30 arcsec Half Energy Width (HEW) and a spectral resolution  $\Delta E/E \lesssim 10\%$  over the whole energy range. Every effort has been made to achieve high collecting area and spectral resolution for the iron line complex  $\sim 7$  keV because of its importance as a diagnostic in Active Galactic Nuclei and clusters of galaxies. Focal plane imaging is provided by passively cooled X-ray sensitive CCD detectors which combine high spatial resolution and good spectral resolution, ( $\Delta E/E \sim 1.5\%$  at 7 keV).

JET-X consists of two identical and coaligned Wolter I X-ray telescopes each made of 12 nested and confocal mirror shells. These shells are 600 mm long and have diameters ranging from 191 to 300 mm, with a focal length of 3500 mm (see Figure 1). The total calculated effective area of each module is 164.6 cm<sup>2</sup> at 1.5 keV and of 72.9 cm<sup>2</sup> at 8.1 keV. The mirror shells were produced by a replication technique utilising a nickel electroforming process which has also used for the SAX instrument<sup>2,3</sup>. An aluminium mandrel is coated with a thin layer of electroless nickel and then superpolished to a surface roughness of  $\lesssim 5$  Å rms. A layer of gold, about 1000 Å thick, is then evaporated on the superpolished mandrel to provide the mirror reflecting surface. The mandrel is then put in an electrolytic bath where a layer of nickel is deposited to a thickness depending on the mirror diameter. Separation of the mirror from the mandrel is effected by cooling the latter since the thermal coefficient of expansion of the aluminium is about twice that of the nickel. Since adhesion of the evaporated gold onto the mandrel is poor but is strong on the electroformed nickel, the gold sticks to the shell. The gold also has high X-ray reflectivity in the energy range 0.3–10 keV.

In this paper we present the results of the acceptance X-ray test for the JET-X Flight Models 1 and 2 (FM1 and FM2) obtained at the PANTER Facility<sup>4</sup> (Neuried, Germany) in January–February 1996.

## 2 FLIGHT MODEL MIRROR UNITS

After the successful mechanical vibration and thermal tests on the Engineering Qualification Model<sup>5</sup> (EQM), the two JET-X flight model units and one flight spare unit were assembled by MEDIALARIO (Bosisio Parini, Italy) under an Agenzia Spaziale Italiana (ASI) contract. The mirror shells for the FMs were replicated from the set of 12 mandrels manufactured by the Company C. Zeiss (Oberkochen, Germany). The replicated set of mirror shells were tested in quasi free standing condition on the UV-optical bench at the Brera Observatory<sup>6</sup>. From these measurements we obtained, after removing the contribution of the diffraction effects, a prediction of the HEW expected at X-ray wavelengths due only to the geometry of the shells. No information concerning the microroughness or short spatial wavelength figuring errors of the mirror can be obtained. In Table 1 we report the results of the UV measurements.

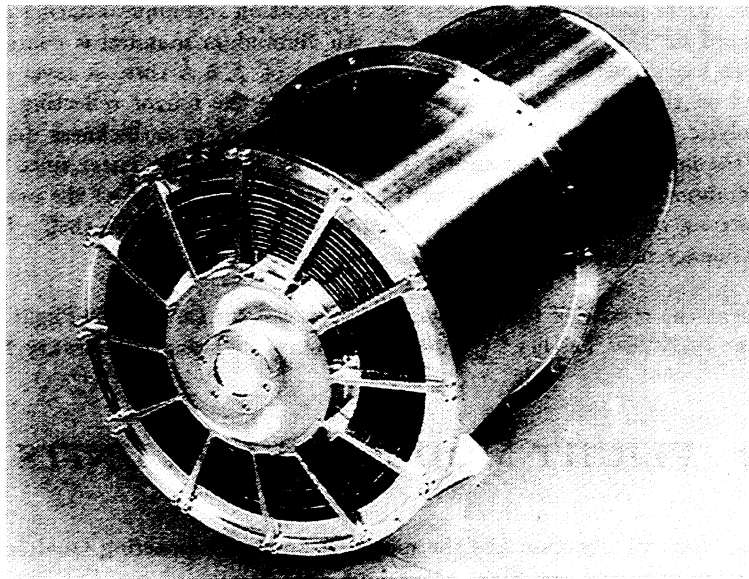
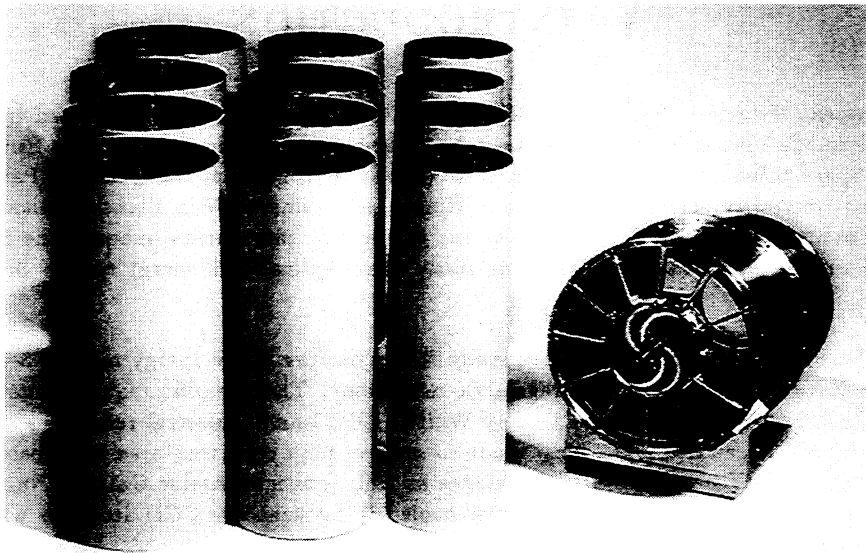


Figure 1: In the upper figure is shown the set of 12 mirror shell and mechanical structure for one model of the optics. In the lower figure is depicted the assembled JET-X FM2.

Table 1: HEW of mirror shells manufactured for the JET-X FM1 and FM2. Measurements on single mirror shells in a quasi free standing condition were made in UV with the vertical bench at 372.5 nm.

| Mirror No. | HEW FM1 arcsec | HEW FM2 arcsec |
|------------|----------------|----------------|
| 1          | 7.2            | 7.3            |
| 2          | 11.8           | 11.8           |
| 3          | 9.3            | 10.2           |
| 4          | 10.9           | 10.1           |
| 5          | 11.7           | 10.3           |
| 6          | 10.8           | 10.7           |
| 7          | 10.4           | 9.4            |
| 8          | 9.9            | 11.2           |
| 9          | 11.9           | 10.6           |
| 10         | 11.2           | 9.7            |
| 11         | 11.4           | 11.0           |
| 12         | 11.7           | 11.9           |

### 3 X-RAY TESTS

The Flight Models (FM1 and FM2) were tested at the PANTER X-ray Facility of the Max Planck Institute für Extraterrestrische Physik, Garching. In this facility a point-like X-ray source is mounted 130 m away from the optics. Inside the test chamber the FM is supported by a translating and tilting stage which allows alignment of the telescope optical axis with the X-ray beam. Two different detectors are mounted on the telescope focal plane: the engineering model of the ROSAT Position Sensitive Proportional Counter<sup>7</sup> (PSPC) and the engineering model of the CCD imaging camera developed at the University of Leicester which will fly on JET-X<sup>8</sup>. Each detector can be centered and focused by means of a remotely controlled three axes manipulator. The measurements in this run were made at 1.5 keV (Al K $\alpha$ ) and 8.1 keV (Cu K $\alpha$ ) for both FM1 and FM2 and at 0.9 keV (Cu L $\alpha$ ) for FM2 only.

#### 3.1 Focal plane detectors

##### 3.1.1 PSPC

The ROSAT PSPC<sup>7</sup> is a multiwire proportional counter with a cathode strip for the position determination. X-rays enter into the detector through a 201 cm<sup>2</sup> circular, 1  $\mu$ m thick polypropylene window additionally coated with carbon and lexan to reduce the UV transmission. These X-rays are then absorbed in the counter volume filled by a mixture of argon, methane and xenon. The window in front of the detector is supported by a rigid circle with 8 equally spaced radial struts. Below this there are a coarse mesh of 100  $\mu$ m tungsten wires with 2 mm spacing and a fine mesh with 25  $\mu$ m tungsten wires with 0.4 mm spacing.

The energy resolution of the PSPC is  $\Delta E/E = 0.43 (E/0.93)^{-0.05}$  (FWHM). The pixel size is 10.87  $\mu$ m  $\times$  10.87  $\mu$ m; the position resolution depends on the energy (e.g. at 0.93 keV is 300  $\mu$ m) and deviates by about 5% over the two degrees field of view. The dead time varies between 170 and 280  $\mu$ s depending on the energy of the

Table 2: HEW and 90% Encircled Energy fraction measurements.

|              | ENERGY  | FM1    | FM2    |
|--------------|---------|--------|--------|
| CCD HEW      | 0.9 keV | –      | 12".9  |
| PSPC 90% EEf | 0.9 keV | –      | 37".4  |
| CCD HEW      | 1.5 keV | 15".1  | 14".6  |
| PSPC 90% EEf | 1.5 keV | 61".5  | 46".6  |
| CCD HEW      | 8.1 keV | 18".7  | 18".8  |
| PSPC 90% EEf | 8.1 keV | 203".5 | 202".9 |

events.

### 3.1.2 CCD

The CCD camera was developed for the XMM EPIC focal plane detector<sup>8</sup>. The device is operated in a frame transfer mode with an image size of  $512 \times 820$  pixels  $27 \times 27 \mu\text{m}$  each. The device is fabricated on high resistivity silicon ( $4000 \Omega \text{ cm}$ ) to extend the high energy response up to 10 keV. The CCD has an open electrode structure to increase the low energy efficiency: a detection efficiency as high as 90% at 1.5 keV is achieved. The CCD is cooled to  $-85^\circ\text{C}$  using liquid nitrogen feed to minimise dark current in the device. Typical frame time is 6 s with a readout noise of 6 electrons (rms). The CCD can be operated in two gain modes: in high gain the device is used to photon count X-rays with an ADC range up to 10 keV; in low gain (10 times reduction) the camera dynamic range is increased to allow X-ray images of the mirror point spread function to be recorded much faster.

## 3.2 Telescope settings

The FMs were aligned first in autocollimation by using an optical laser beam in connection with a reference mirror mounted in front of the telescope. A further alignment was obtained looking at the symmetry of the ring produced by X-rays reflected only onto the first mirror surface which fall inside the PSPC sensitive area. This effect is due to the divergent beam of the source which is 130 m away. An estimated accuracy of about  $10''$  can be obtained. The optimum focal position was then found by moving the detectors along the Z axis: in the case of the CCD the images were evaluated at  $-10, -6, -4, -2, -1, 0, 1, 2, 4, 6, 10$  mm from the position of the nominal focus. The same focal position was found at 1.5 and 8.1 keV for both FM1 and FM2 to within a fraction of millimeter.

## 3.3 Half Energy Width and Encircled energy fraction measurements

The spatial resolution of the JET-X mirrors is about the same as the PSPC detector. Therefore the HEWs were only derived from the CCD measurements<sup>9</sup>. On the other hand the CCD area is too small (especially at high energies) to allow a correct determination of the 90% Encircled Energy Fraction (EEF), due to the scattering of

the optics. In this case the PSPC provides more reliable values (see Table 2). The results of the HEW measured for the FM1 and FM2 and of the 90% EEf are reported in Table 2.

The HEW for the nest expected from the UV measurements of individual shells is  $\sim 11$  arcsec. The low energy X-ray measurements are just 2 arcsec worse than this indicating that the angular resolution is limited by the figuring of the shells and not distortions introduced by integration of the shells into a nest.

Additional measurements were performed to characterise the angular resolution of the FMs. With the CCD in the focal plane we took a double exposure moving the detector by the equivalent of 20 arcsec after half the exposure time. This provided us with a simulation for two sources of the same intensity separated by 20 arcsec. At both 1.5 and 8.1 keV the two sources are well resolved, underlining the excellent angular resolution of JET-X (see Figure 2).

### 3.4 Effective Area

The geometric collecting area of each FM is  $231.1 \text{ cm}^2$ . The divergence of the Panter Facility X-ray beam causes a loss of area because of the lack of secondary reflection for some photons. This loss amounts to 5%. The twelve arms spider causes a decrease of the useful area of 10%, so that the utilised geometrical area of JET-X FM units at PANTER is  $196.7 \text{ cm}^2$ .

Effective area measurements were made with the PSPC and the CCD. For the PSPC, measurements were performed at different intra-focal position (0, -20, -40, -60, -80, -100 mm) together with a scanning exposure at -40 mm (intra-focus). This strategy was adopted in order to minimise the effects of the PSPC meshes. The CCD images were taken with the source defocused by -100 mm (intra-focus) in order to avoid the pile-up of photons at the centre of the focused distribution.

To measure the effective area first the FM is illuminated by the X-ray beam and the detector in the focal plane collects the reflected photons. The detector is then exposed directly to the incoming beam (flat field). The effective area is calculated as the ratio between the exposure and flat field counts, multiplied by the sensitive area of the detector. A correction factor taking into account the different distance from the source to the telescope entrance and to the detector is also applied. Figure 3 shows the on-axis effective area vs. energy obtained with a ray-tracing simulation together with the values obtained from the measurements.

The PSPC and CCD gave different results for the JET-X effective area; this is probably due to a stability

Table 3: PSPC Effective area measurements for FM1 and FM2.

| ENERGY<br>(keV) | FM1<br>$\text{cm}^2$ |                 | FM2<br>$\text{cm}^2$ |                 | Theory <sup>†</sup><br>$\text{cm}^2$ |          |
|-----------------|----------------------|-----------------|----------------------|-----------------|--------------------------------------|----------|
|                 | 130 m                | $\infty$        | 130 m                | $\infty$        | 130 m                                | $\infty$ |
| 1.49            | $150.0 \pm 1.0$      | $158.9 \pm 1.1$ | $152.0 \pm 0.8$      | $161.0 \pm 0.8$ | 155.4                                | 164.6    |
| 8.05            | $58.3 \pm 0.5$       | $69.2 \pm 0.6$  | $58.5 \pm 0.5$       | $69.5 \pm 0.6$  | 61.4                                 | 72.9     |

The quoted error derives from the counting statistics.

<sup>†</sup> Theoretical values for the effective area has been derived from the latest Henke reflectivity tables.

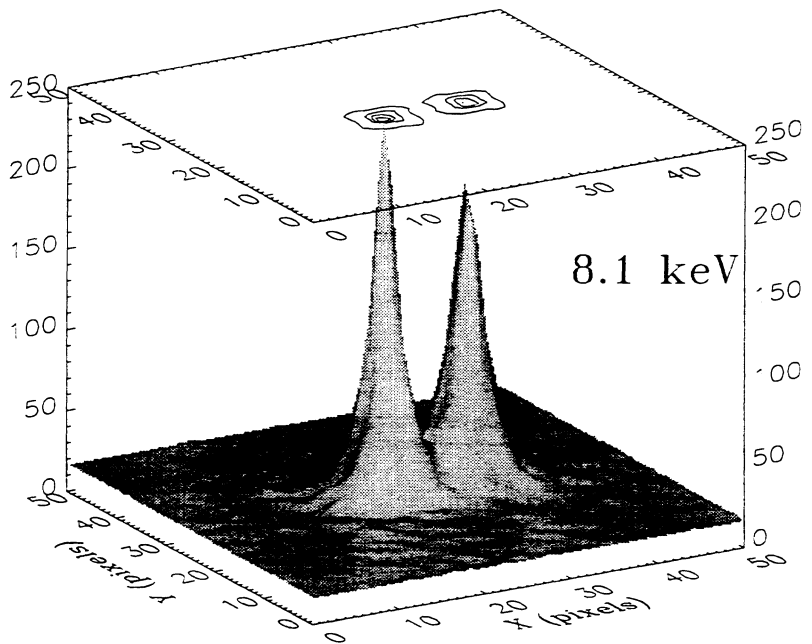
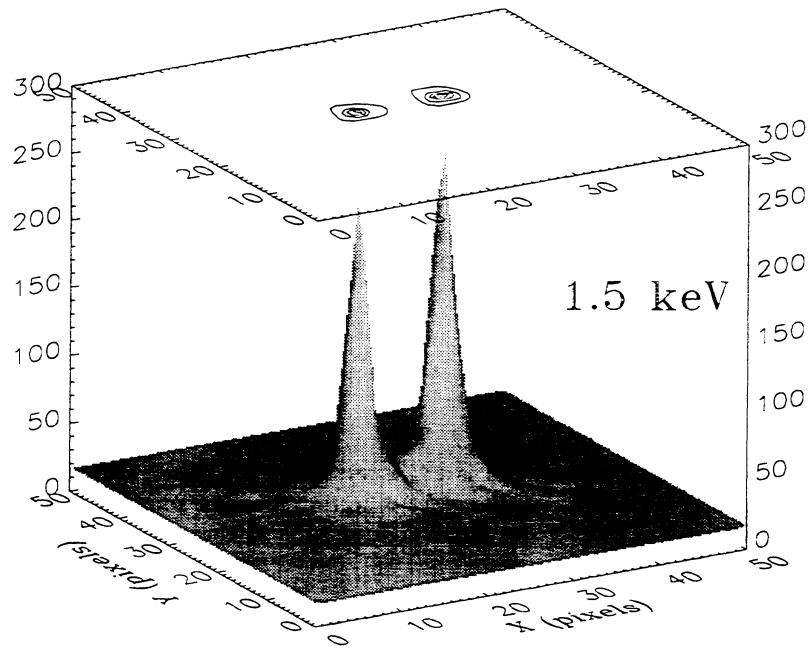


Figure 2: JET-X FM2 CCD images of two sources separated by 20 arcsec at 1.5 keV (upper figure) and 8.1 keV (lower figure).

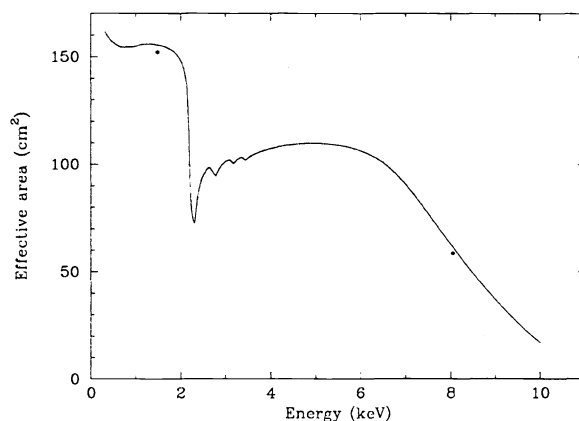


Figure 3: Theoretical effective area at the PANTER test facility. The two points represent the measurements on JET-X FM2 at 1.5 and 8.1 keV.

problem of the X-ray source. Measurements with the Flight Spare model (FM3, May 1996) showed that variations in the source count rate by more than 20% in an hour can be observed during a day of measurements. The FM1 and FM2 runs were performed without the aid of a monitor counter controlling the source stability. For this reason CCD measurements, which require very long exposure times for the flat fields (of the order of a few hours) are not so reliable. The experience with the FM3 showed us that the monitor counter correction is extremely important in the case of the CCD; for the PSPC this correction is important only during strong source variations. The PSPC and CCD effective area measurements made later for the FM3 model with the aid of the monitor counter, agree within the statistical errors.

In Table 3 we present only PSPC measurements for which the source stability problem is minor because of the smaller exposure time. We can conclude that the effective area of the FM1 and FM2 are  $-3.5\%$  and  $-2.2\%$  at 1.5 keV lower than the theoretical value, respectively; at 8.1 keV these are  $-5.0\%$  and  $-4.7\%$  lower. (For the FM3 the losses are about  $-2\%$  at 1.5 keV and  $-5\%$  at 8.1 keV using both CCD and PSPC measurements).

### 3.5 Surface roughness

The calibration data from the JET-X flight mirrors recorded with the PSPC and CCD detectors at the PANTER facility indicate that the scattering wings of the Point Spread Function have a very low surface brightness even at 8 keV. By using first order scattering theory in the smooth surface limit we can predict the scattering wings expected from these surface height deviations<sup>10</sup>. A power law surface roughness power spectrum with specific roughness of  $25 \text{ \AA}^2 \text{ mm}$  and a power-law index of 1.4 provide the best fit to the PSPC data for the JET-X FMs. The rms roughness of the fit (obtained by integrating the power law) is  $\sigma \sim 3.5 \text{ \AA}$  for spatial wavelengths  $< 10 \mu\text{m}$ .

The collecting area losses at 1.5 keV are expected to be totally dominated by geometrical misalignments etc., while the larger losses at 8.1 keV are introduced by X-ray scattering so the collecting area measurements indicate a scattering loss of  $-2.5\%$  at 8.1 keV. This is expected from a surface roughness of  $\sim 3 \text{ \AA}$  which is entirely consistent with the analysis of the scattering wings.



## 4 CONCLUSIONS

The acceptance X-ray tests for the JET-X FMs were successful. The HEWs are well within the required specifications over the whole energy range and are dominated by figuring errors in the individual shells and not the surface quality or the integration of the shells into a Wolter I nest. Effective area measurements reveal small losses with respect to the theoretical values ( $\lesssim 5\%$ ), comparable to what shown by SAX LECS and MECS mirrors. A simple estimate of the surface roughness has been obtained using the first order scattering theory: we derive a rms roughness of  $\sigma \sim 3.5 \text{ \AA}$ , well within the scientific requirements and consistent with the loss in effective area.

The final end-to-end calibration test for the JET-X FMs are now planned for fall 1996.

## 5 ACKNOWLEDGEMENTS

We wish to thank G. Boella, G. Chincarini and L. Scarsi for supporting and encouraging our work. We thank U. Bergamini, M. Casiraghi, G. Castelli, G. Crimi, D. Garegnani, A. Mistò, A. Salini, R. Valtolina from the OAB for the technical assistance during various phases of the project. The technical contribution of P. Cerutti, R. Graue, G. Valsecchi and R. Villa from MEDIALARIO has been very much appreciated. Special thanks go to P. Cecchini, B. Negri and G. Rossetti from the Agenzia Spaziale Italiana (ASI) for their valuable assistance in running the contract between ASI and MEDIALARIO.

This work was carried out under a contract from ASI.

## 6 REFERENCES

- [1] A. Wells, D.H. Lamb, K.A. Pound, G.C. Stewart, B. Aschenbach, H. Braüninger, G. Hasinger, J. Trümper, O. Citterio, L. Scarsi, A. Peacock, B. Taylor, "JET-X a Joint European X-ray Telescope for Spectrum-X", IAU Coll. N. 115, Massachusetts, (1988).
- [2] O. Citterio, G. Bonelli, G. Conti, E. Mattaini, E. Santambrogio, B. Sacco, E. Lanzara, H. Braüninger, W. Burkert, "Optics for the X-ray imaging concentrators aboard the X-ray astronomy satellite SAX", Appl. Opt. 27, 1470, (1988).
- [3] O. Citterio, P. Conconi, M. Ghigo, R. Loi, F. Mazzoleni, E. Poretti, G. Conti, T. Mineo, B. Sacco, H. Braüninger, W. Burkert, "X-ray optics for the JET-X experiment aboard the SPECTRUM-X satellite", Proc. SPIE 2279, 480, (1994).
- [4] B. Aschenbach, H. Braüninger, K.H. Stephan, J. Trümper, "X-ray test facilities at Max Plank Institute, Garching", Proc. SPIE 184, 234, (1979).
- [5] O. Citterio, P. Conconi, M. Ghigo, F. Mazzoleni, E. Poretti, G. Conti, G. Cusumano, B. Sacco, H. Braüninger, W. Burkert, "Status of the qualification model of the X-ray optics for the JET-X telescope aboard the Spectrum-X Gamma satellite", Proc. SPIE 2515, 44, (1995).
- [6] P. Conconi, U. Bergamini, O. Citterio, G. Crimi, M. Ghigo, F. Mazzoleni, "Evaluation by UV optical measurements of the imaging quality of grazing incidence X-ray optics", Proc. SPIE 2011, 89, (1993).
- [7] U. Briel, E. Pfefferman, "The Position Sensitive Proportional Counter (PSPC) of the ROSAT telescope", Nucl. Instr. and Meth. A242, 376, (1986).

- [8] A. Owens et al., "The X-ray CCDs developed for the Joint European X-ray Telescope", *Journal of X-ray Science and Technology*, in press, (1996).
- [9] C.M. Castelli, H. Braüninger, W. Burkert, R. Egger, S. Campana, G. Cusumano, A. Wells, R. Willingale, "Use of the X-ray CCD in calibration of the flight mirrors for the JET-X telescope for Spectrum X- $\gamma$ ", *Proc. SPIE 2808*, in press (Denver 1996).
- [10] E.L. Church, H.A. Jenkinson, J.M. Zavada, "Measurement of the finish of diamond-turned metal surfaces by differential light scattering", *Opt. Eng.* 16, 360, (1977).